

<b>REPORT DOCUMENTATION PAGE</b>			Form Approved OMB No. 0704-0188	
Public reporting burden for this collection of information is estimated to average 1 hour per response, including the time for reviewing instructions, searching existing data sources, gathering and maintaining the data needed, and completing and reviewing the collection of information. Send comments regarding this burden estimate or any other aspect of this collection of information, including suggestions for reducing this burden, to Washington Headquarters Services, Directorate for Information Operations and Reports, 1215 Jefferson Davis Highway, Suite 1204, Arlington, VA 22202-4302, and to the Office of Management and Budget, Paperwork Reduction Project (0704-0188), Washington, DC 20503.				
1. AGENCY USE ONLY (Leave blank)		2. REPORT DATE 2/2/2000		3. REPORT TYPE AND DATES COVERED Final Progress Report
4. TITLE AND SUBTITLE Strength-Structure-Chemistry Relationship for Metal/Ceramic, Metal/Polymer and Ceramic/Ceramic Interfaces			5. FUNDING NUMBERS DAAH04-96-1-0010	
6. AUTHORS  V. Gupta				
7. PERFORMING ORGANIZATION NAME(S) AND ADDRESS(ES)  UCLA, Los Angeles, CA 90095			8. PERFORMING ORGANIZATION REPORT NUMBER	
9. SPONSORING/MONITORING AGENCY NAME(S) AND ADDRESS(ES)  U.S. Army Research Office P.O. Box 12211 Research Triangle Park, NC 27709-2211			10. SPONSORING/MONITORING AGENCY REPORT NUMBER  ARO 35104.9-M5	
11. SUPPLEMENTARY NOTES				
12a. DISTRIBUTION/AVAILABILITY STATEMENT  Approved for public release; distribution unlimited.			12b. DISTRIBUTION CODE	
13. ABSTRACT (Maximum 200 words)  This ARO-funded program was unusually successful as it accomplished much beyond the proposed goals of (1) uncovering of basic molecular and microstructural-level mechanisms that govern adhesion between dissimilar metal and ceramic components in film/substrate geometry; (2) development of an interface tensile strength data base; (3) development of two novel toughness-measuring tools, leading to hitherto unreported basic toughness data, the absence of which had blocked the further development of first principle calculations for understanding adhesion; (4) the latter measurements were also used to confirm the fundamental nature of the tensile strength data obtained by the laser spallation experiment, and its relation to the data obtained by other techniques. In addition, the program culminated into (a) technology development that led to the use of the laser spallation concept, and its transfer in few cases, to companies worldwide, belonging to different industries, such as semiconductor (Intel Corporation, Hitachi, Dow Corning Corporation), automobile (Delco), television (LG Gould in Korea), biomedical (Pacesetter Inc., Baxter Corporation), aircraft engines (Pratt and Whitney, Westinghouse Corporation), paint (Du Pont), and Dentistry, (c) use of technology for addressing new basic problems in different disciplines, such as biomedical (treatment of arrhythmias, and dissolution of body fat), earth sciences, ice mechanics (newer-types of hydrophobic coatings), and (d) recording of the highest interface crack speeds which now has questioned the well-established dynamic fracture frameworks.				
14. SUBJECT TERMS  Interface Strength, Metal/Ceramic Interfaces, Laser Spallation Technology, Microelectronic Devices and Packages, Jet Aircraft Engines, Interface Toughness, Deicing, Biomedical, Dynamic Fracture			15. NUMBER OF PAGES 23	
			16. PRICE CODE	
17. SECURITY CLASSIFICATION OF REPORT	18. SECURITY CLASSIFICATION OF THIS PAGE	19. SECURITY CLASSIFICATION OF ABSTRACT	20. LIMITATION OF ABSTRACT	

NSN 7

puter Generated

STANDARD FORM 298 (Rev 2-89)  
Prescribed by ANSI Std Z39-18  
298-102

20000707 025

THIS QUALITY INSPECTED 4

## Table of Contents

SECTION	Page Number
Form 298	i
Table of Contents	1
List of Illustrations and Tables	2
FINAL PROGRESS REPORT DESCRIPTION	
1. Problem Statement	3
2. Overall Accomplishments	3
3. The Basic Laser Spallation Technique	4
4. Progress Report	4
4.1 Development of Adhesion Metrology Tools and their Assessment	4
4.1.1. Multilayer Testing	
4.1.2. In-situ Testing at Elevated Temperatures	
4.1.3. Measurements at Cryogenic Temperatures	
4.1.4. Measurement of Interface Toughness	
4.2. Generation of Adhesion Data-Base and Understanding of the Basic Adhesion Mechanisms for Selected Technologically-Important Systems	7
4.2.1. Basic Parameters Affecting Adhesion of Metal/Ceramic Interfaces	
4.2.2. Multilayer Microelectronic Systems	
4.2.3. Effect of Film Thickness and Cure Temperature on the Cracking Behavior of Low-k Dielectric Films	
4.3. Technology Transfer	10
4.4. Contributions to other Fields	11
4.4.1 Biomedical	
4.4.2. Dynamics Fracture/Geophysics	
5. List of Publications and reports	13
6. List of Participating Scientific Personnel	14
7. Bibliography	15
8. Figures and Tables	16

## List of Illustrations

Figure 1. Schematic of the laser spallation experiment, along with that of the interferometer used to record free surface velocities.

Figure 2. Stress wave profiles in Si at different laser fluences.

Figure 3. Conversion chart for reducing the laser fluence into peak stress wave amplitudes in Si.

Figure 4. Interface stress histories at interfaces in a Si/Si<sub>3</sub>N<sub>4</sub>/polyimide system, as calculated using a finite difference program, with the stress history in Si as input.

Figure 5. A schematic of the apparatus used for measuring interface strengths at elevated temperatures.

Figure 6. A schematic of the apparatus used for measuring interface strengths at cryogenic temperatures, along with ice/Al strength data.

Figure 7. Forced buckling profiles as viewed under an optical microscope, along with the quantification of their curvatures using an atomic force microscope. The interface toughness data obtained for selected metal/ceramic interface system is shown in Fig. 8.

Figure 8. Collection of figures demonstrating the interface toughness-measuring technique that uses a laser-generated stress wave to initiate a photolithographically-induced interface crack. The toughness data for selected interface system is shown in the table.

Figure 9. Collection of figures demonstrating the measured anisotropy in the interface strength across a Nb/sapphire interface, both in terms of the measured numbers, and patterns left behind by the spalling Nb film.

Figure 10. Table showing interface strength for few metal/Si interface systems.

Figure 11. A typical interface delamination observed prior to coating spallation by observing optical fringes under an optical microscope.

Figure 12. The effect of in-situ temperature rise on the tensile strength of polyimide/nitride interface. Also shown is the data for samples that were tested after cooling to ambient.

Figure 13. The effect of varying relative humidity on the tensile strength of polyimide/nitride interface for samples held for 48 hrs inside a humidity chamber maintained at 38°C.

Figure 14. The effect on interface strength of exposing the samples to a 60% RH and 38°C environment for increasing duration.

Figure 15. The effect on interface strength of exposing the samples to a 60% RH environment for a fixed time (24 hrs) at different temperatures.

Figure 16. Schematics demonstrating results of using laser ultrasound in two biomedical applications.

Figure 17. A collection of figures demonstrating the interface-crack-speed-measuring procedure and results.

## 1. Problem Statement

Measurement and control of interface tensile strength and toughness is an important fundamental problem, which impacts many modern technologies, such as those related to the development of tough composite materials, and longer-lasting corrosion-resistant, thermal barrier, tribological, and electronic coatings.

The aim of this work was to understand how different surface variables and coating deposition parameters influence the fundamental adhesion of metal and ceramic films on engineering substrates, using a previously-developed laser spallation technique capable of measuring the tensile strength of interfaces. Additionally, the fundamental nature of the data obtained by the latter was to be examined by relating it to the intrinsic interface toughness, which in turn was to be measured independently by developing novel experiments. Finally, the extension of the laser spallation strategy for testing adhesion in multilayer assemblies was sought because of its importance to the paint, aircraft engine, and electronic device industries.

## 2. Overall Accomplishments

This ARO-funded program was unusually successful as the accomplishments were much beyond the proposed goals. This work resulted in (a) fulfillment of the program objectives which included, uncovering of basic molecular and microstructural-level mechanisms that govern adhesion between dissimilar metal and ceramic components in film/substrate geometry; development of an interface tensile strength data base for important engineering bimaterial systems, including dielectric/semiconductor interfaces; development of two novel toughness-measuring tools, one a control delamination technique, and the other based on shock wave loading of photolithographically-generated microcracks, which led to hitherto unreported basic toughness data, the absence of which had essentially blocked the further development of first principle calculations for understanding adhesion; the latter measurements were also used to confirm the fundamental nature of the tensile strength data obtained by the laser spallation experiment and hence the data obtained by other competing techniques, (b) technology development that led to the use of the laser spallation concept, and its transfer in few cases, to companies worldwide, belonging not to one but different industries, such as semiconductor (Intel Corporation, Hitachi, Dow Corning Corporation), automobile (Delco), television (LG Gould in Korea), biomedical (Pacesetter Inc., Baxter Corporation), aircraft engines (Pratt and Whitney, Westinghouse Corporation), paint (Du Pont), and Dentistry (improved Ti implants with highly adherent calcium-phosphate coating), (c) the laser ultrasound technology being used for addressing basic problems in different disciplines, such as biomedical (treatment of arrhythmias, and dissolution of body fat), earth sciences and dynamic fracture (use in the determination of interface crack speeds, with applications to fault instability), ice mechanics (development of strength measuring apparatus at cryogenic temperatures, and subsequent development of newer-types of hydrophobic coatings), and finally, (d) recording of the highest interface crack speeds which now has questioned the well-established dynamic fracture frameworks.

A brief description of the various accomplishments listed above is provided below after introducing the laser spallation experiment.

### 3. The Basic Laser Spallation Technique

In this experiment (Fig. 1), a 2.5 nanosecond (ns) long Nd:YAG laser pulse is made to impinge over a 3 mm-dia area on a 0.3  $\mu\text{m}$ -thick aluminum film which is sandwiched between the back surface of a substrate disc and a 50 to 100  $\mu\text{m}$  thick layer of solid waterglass. The melting-induced expansion of aluminum under confinement generates a compressive stress pulse (with 1 nanosecond rise time) directed toward the test coating which is deposited on the substrate's front surface. The compressive stress wave reflects into a tensile pulse from the coating's free surface and leads to its spallation (complete removal) at a sufficiently high amplitude. The critical stress at the interface is calculated by measuring the transient displacement history of the coating's free surface (induced during pulse reflection) by using an optical interferometer with a resolution of only 0.2 ns in the single shot mode. The measured free surface velocity is related to the local interface stress via a wave mechanics-based simulation. An expanded discussion on this technique and why it provides a fundamental measure of the interface's tensile strength, including its correlation with the atomic structure and interfacial chemistry, can be found elsewhere [1-3].

### 4. Program Accomplishments

For the sake of convenience, the overall accomplishments are divided into four groups, viz., (1) Development of adhesion metrology tools and their assessment, (2) Generation of adhesion database and understanding of basic adhesion mechanisms in selected technologically-important systems, (3) Technology transfer, and (4) Contributions to other fields.

#### 4.1. Development of Adhesion Metrology Tools and their Assessment

This involved the extension of the laser spallation concept for measuring tensile strength of interfaces in planar multilayer assemblies, and in-situ at cryogenic (up to  $-40^\circ\text{C}$ ) and elevated temperatures (up to  $1000^\circ\text{C}$ ).

##### 4.1.1. Multilayer Testing

This development was motivated by applications in the electronic device industry. The new procedure is exemplified on a Si wafer/ $\text{Si}_3\text{N}_4$  (750 nm-thick)/polyimide (4-5  $\mu\text{m}$ -thick) multilayer system, even though the procedure is general and applicable to other material combinations.

The basic laser spallation methodology as discussed above for a single film/substrate interface system was adopted. While applying the technique to multilayers supported on a Si chip, it was found that sufficient tensile stress for decohering interfaces could be generated without the use of the laser absorbing Al film. So no Al layer was used for the Si system. However, as before, it was still necessary to cover the Si bare surface opposite to that carrying the multilayers with a 40-50  $\mu\text{m}$ -thick layer of waterglass. The laser heating diameter (3 mm) to substrate thickness ( $< 1\text{ mm}$ ) always exceeded 3. As discussed in Argon *et al.* [4], this ensures one-dimensionality of the stress wave over 95% of the stressed interface area.

For the sake of convenience and also for testing multilayer samples, the following three-step procedure was adopted [5]. The critical laser fluence causing coating spallation was recorded first. Quantification of interface stress followed next. Simultaneous recording of the free surface velocity of the separating film, using interferometry, was not performed in the present work. Instead, stress pulses were quantified as a function of laser fluence inside a bare Si wafer bearing the same thickness, structure, and orientation, and with the same waterglass layer thickness as in

actual test specimens with multilayers. The procedure used to record and reduce the fringe data to actual stress wave profiles was otherwise similar to that used previously [1]. The resulting stress wave profiles at different laser fluences in a Si wafer are shown in Fig. 2. The rather sharp rise time (1-2 ns) and duration (~10 ns) of the stress wave is notable, and so is the similarity in their profiles at different laser fluences. The peak amplitude of the stress pulses was recorded as a function of the laser fluence and waterglass layer thickness. Figure 3 shows such a chart, which essentially allows the conversion of the laser fluence to stress pulse amplitude inside Si for a given waterglass layer thickness. Finally, a finite element-based acoustic wave mechanics simulation was developed which calculates the tensile stress histories at any of the interfaces in a given multilayer assembly when loaded normally by the propagating stress wave of a prescribed profile and amplitude from the Si side. Other inputs to the program include, thickness of each layer, and their respective elastic properties, including density, Young's modulus, and Poisson's ratio. Only one wave profile was considered in the simulation, as all stress wave profiles at different laser fluences reduced to a single one when normalized by the peak amplitude. Thus, it was only necessary to use the peak wave amplitude as the loading parameter, which in turn could be read off from Fig. 3 corresponding to the threshold laser fluence.

With the above three-step procedure, it was no longer necessary for the interferometric measurements to be performed during each spallation event. The threshold laser energy for coating spallation was determined (which takes only a few seconds) using visual inspection of the shock-loaded samples, and converted to the peak stress pulse amplitude using Fig. 3 for the appropriate waterglass layer thickness. The normalized stress wave profile with this amplitude was used as an input to the program along with the prescribed multilayer geometry and elastic properties to calculate the desired tensile stress history at the interface at which failure was observed. Figure 4 shows the results of a typical simulation showing the calculated interface stress histories at the nitride/polyimide and nitride/oxide interfaces. Positive values represent tensile stresses. The peak of the interface tensile stress history was taken as the interface strength. Specific interface strength results are presented in Section 4.2.

#### ***4.1.2. In-situ Testing at Elevated Temperatures***

This development was motivated by the desire to understand if irreversible structural changes can lead to adhesion degradation in thermal barrier coatings and multilayer electronic devices, during operation. Again, this new procedure is demonstrated on the multilayer system considered above.

The basic mechanics of the laser spallation experiment discussed above remains the same even at elevated temperatures [6]. The overall experimental assembly showing the above sample inside an oven with an in-house built vacuum system is illustrated in Fig. 5. The oven is capable of maintaining a temperature anywhere between the ambient and 1200°C even though the maximum temperature for the present tests was limited to 150°C. The sample was supported vertically inside a groove made on a pyrolytic graphite plate. The plate was slid inside the quartz tube to position the sample more or less at the center of the heating zone. The two ends of the quartz tube were capped with identical quartz window-stainless steel assembly systems so as to allow access to the YAG and Argon ion laser beams used for pulse generation and recording, respectively.

A long focal length lens was used to direct the YAG laser beam from the outside to a 3 mm diameter spot on the confined Si surface opposite the polyimide layer. After the sample was left inside the oven long enough (10-15 min) to reach equilibrium conditions, the interface was loaded with single stress pulses of increasing amplitudes at different locations (to avoid fatigue effects) to



find the threshold stress pulse causing coating spallation. The quantification of the interface stress corresponding to the latter followed the procedure outlined above. Specific interface strength results are presented in Section 4.2.

#### 4.1.3. Measurements at Cryogenic Temperatures

An environmental cell was built to carryout in situ measurements at cryogenic temperatures, as needed to study ice adhesion on structural surfaces. This apparatus (Fig. 6) involved a plexiglass housing which was maintained at the test temperature by flow of pre-cooled air, which was supplied in a Cu tube immersed in liquid nitrogen. Two specially-constructed windows that disallowed condensation of the air from the outside, were provided on the front and back faces of the housing to communicate with the shock-wave-generating YAG laser pulse and the interferometric He-Ne laser beam. Samples of Al disc, with ice grown on them in an external walk-in cooler and maintained at  $-10^{\circ}\text{C}$  were transferred to the housing and taken to the test temperature prior to the test. Other test procedures, including quantification of the ice/Al interface strength were essentially the same as discussed above. Figure 6 provides hitherto unreported tensile strength data for ice/Al interfaces. Other details can be found elsewhere [7], and also in Section 4.2, where the development of a new ice adhesion mitigating self-assembled monolayer (SAM) of dimethyl-n-octadecylchlorosilane, is discussed.

#### 4.1.4. Measurement of Interface Toughness

Besides interface strength, the mechanical response of the interface can also be characterized in terms of intrinsic toughness (energy required to fracture an interface). In fact, in many applications, the interface failure is due to growth of pre-existing flaws which makes the interface toughness as a more appropriate parameter for mechanical characterization. This property was obtained by two novel techniques, developed as part of this ARO-funded program.

##### *Control Delamination Technique*

If the residual stresses in the deposits are not too high then the spontaneous delamination of the coatings will not occur. Thus, independent measurements of coating residual stress, film modulus, and its critical thickness, cannot be used to calculate the interface toughness [8]. In such cases, the coatings were forced to buckle from the substrates by depositing a highly strained layer of Nb on top of the test coating (Fig. 7 shows a collection of illustrations demonstrating the experimental procedure). The thickness of this top Nb layer is carefully controlled till it buckles the lower test coating away from the substrate. The intrinsic strain in the Nb loading layer is recorded independently by measuring its buckled profile  $y(x)$  which leads directly to its intrinsic strain  $\varepsilon_0$  by using the elementary formula

$$\varepsilon_0 = \left( \frac{1}{1+\nu} \right) \frac{1}{4L} \int_{-L}^L y'^2(x) dx ,$$

where prime denotes the derivative and  $\nu$  is the Poisson's ratio for the coating material. Physically, the above formula takes the difference between the buckled (relaxed) length of the coating strip and its straight length  $2L$  which it occupies when residually stressed under compression so as to fit flat on the substrate. When combined with the critical thickness  $t$  at

which the bilayer buckles, toughness of test coating/substrate interface can be readily calculated from,

$$G = \frac{1 + \nu}{2(1 - \nu)} t E \varepsilon_o^2.$$

Here  $E$  is elastic modulus of the coating material. This test will not work if the Nb/test coating interface comes apart, but so far we have yet to find a system where this actually occurs. Details of this technique can be found in Pronin and Gupta [9].

#### *Intrinsic Toughness using Laser-Generated Stress Pulses*

This technique which is demonstrated schematically in the sequence of figures collected as Fig. 8, is described in details in [10]. In this technique an aluminum strip of 100  $\mu\text{m}$  width and 100  $\text{\AA}$  thickness is orthogonally overlaid by the test coating of interest. Aluminum is dissolved in an etchant to which the test coating is neutral. This leaves an interface crack of well-defined geometry underneath the test layer. The crack is loaded by a stress pulse which is generated in-line with the flaw and on the back surface of the substrate by using the laser spallation assembly. The critical free surface velocity of the test coating at crack initiation is recorded by using an optical interferometer, and related to the crack initiation energy (or interface toughness) by using a numerical simulation based on dynamic fracture. Quite remarkably, the numbers obtained from this technique were quite close to those obtained from the controlled delamination technique even though the loading strategies are quite different (see Table listed in Fig. 8). Also all these numbers are less than 1  $\text{J/m}^2$  and thus, within the expected range of intrinsic toughness values. The advantage of this technique, however, is for systems characterized by rather high interface strengths such that they cannot be pulled apart by any loading layer. Clearly this technique will always work since the crack driving force can be brought down at will by simply enlarging the initial crack size.

### **4.2. Generation of Adhesion Data-Base and Understanding of the Basic Adhesion Mechanisms for Selected Technologically-Important Systems**

#### **4.2.1. Basic Parameters Affecting Adhesion of Metal/Ceramic Interfaces**

The effects of substrate orientation (basal: 1.0 GPa vs. prismatic: 1.7 GPa), substrate cleanliness (chemical vs. backscatter cleaning), substrate roughness (alumina: 280 MPa vs. sapphire: 1-1.7 GPa) and coating deposition mode (RF: 1.5 GPa vs. DC: 0.9 GPa sputtering) on the tensile strength of Nb coatings/sapphire interfaces was quantified. Remarkably strength anisotropy along different crystallographic directions of sapphire was realized in terms of different spallation patterns left behind by the coating. A model that explained the observed anisotropy in strength was also developed, which beside explaining successfully the quantitative differences in the interface strength across prismatic and basal sapphire orientations was also able to predict the spallation patterns. These results along with the table summarizing the measured interface strength values are collected in Fig. 9. Other details of the investigation, including sample and substrate preparation, can be found in [11].

The intrinsic toughness data obtained by the two novel techniques is presented in Fig. 8. It was found that the intrinsic toughness data from both techniques related rather well with the



tensile strength numbers for the Nb/sapphire interface system through previously characterized TEM microstructures of the interfacial region. All these parameters were found to be correlated, and thus, provided proof for a previously-developed intrinsic strength-toughness relationship by the PI [1]. This shows the fundamental nature of the measurements provided by both the interface strength and toughness-measuring techniques, developed as part of this ARO-funded program.

#### **4.2.2. Multilayer Microelectronic Systems**

Figure 10 shows interface strength data for few metal films deposited on a Si wafer. A fundamental investigation was also carried out to understand the mechanisms of interface adhesion, and its degradation when exposed to controlled amounts and duration of humidity and in-situ temperature rise, in a Si/nitride/polyimide system. These results, which are first of their kind, are discussed in details below and contained in manuscripts [12]&[13]. Dramatic implications of these measurements for device reliability are also discussed at the end.

Failure in all samples, whether tested in-situ at elevated temperatures or those subjected to moisture and humidity treatment alone were all at the nitride/polyimide interface. Interestingly, because of the transparency of the polyimide film, the threshold laser energy that caused the nucleation of first interface crack or onset of decohesion in an otherwise intact film could be spotted by viewing Newton fringes under an optical microscope, much prior to complete removal of the coating from the substrate. Figure 11 shows an example of such a failure.

In-situ elevated temperature test results are summarized in Fig. 12. The strength degrades non-linearly from 304 MPa at 22°C to 245 MPa at 50°C, beyond which it degrades almost linearly with the temperature to 167 MPa at 150°C. It is interesting to note that only a single heating cycle was sufficient to cause irreversible degradation in the interface strength as evidenced by ambient testing of samples that were heat-treated at 50°C and 150°C for 10 min and cooled in air. As figure 8 shows the strength reduced dramatically to 167 MPa compared with 304 MPa for the 50°C, and this effect was even stronger in samples that were cooled from 150°C where the strength reduced to only 141 MPa. A plausible reason for this degrading effect is furnished later.

Figure 13 shows the effect of varying relative humidity when the samples were held for 48 hrs at 38°C. There is a strong degrading effect of moisture between 50% and 60% RH beyond which the effect attains a saturation level. Uncovering of this saturation effect is of obvious importance in the design and prediction of device reliability.

The degrading effect of subjecting the samples to increasing durations in a fixed moisture (60% RH) and temperature (38°C) environment is shown in Fig. 14. The effect does not appear to follow the typical Arrhenius-type as is usually expected in such studies. Instead, there is almost a linear degradation from 224 MPa at 24 hrs hold to 195 MPa at 72 hrs hold time, beyond which the strength plunges significantly to 140 MPa at times nearing 100 hrs. Clearly, such points where the data shows a dramatic turn should be critical while designing packages and IC's using the proposed new reliability strategy.

Figure 15 shows the effect of the temperature (30°C, 35°C and 40°C) at which samples were exposed in a 60%RH environment for a fixed time (24 hrs). This matrix of temperatures was chosen since previous in-situ tests showed the degrading effect to be the most significant in

this temperature range. The data in Fig. 15 shows a steeper decrement of strength with temperature compared with samples that were not exposed to with humidity environment.

### *Discussion*

It is generally known that the variables of moisture, temperature and time degrade interfacial adhesion, this work is the first that quantifies such effects in the fundamental strength of interfaces. Even though a one-on-one correlation of the degraded strength with the corresponding change in the interfacial chemistry and structural relaxations is outside the scope of the present investigation, a plausible mechanism for the observed strength variations is suggested below.

The chemical structure of the as-spun polyimide precursor shows two open carbon rings. During baking, ring closure occurs on account of dehydrolysis and results in the formation of the stable polyimide molecule. Since nitrogen in  $\text{Si}_3\text{N}_4$  has a lone pair of electrons, it can form hydrogen bonds at one of the open ring sites of the precursor molecule, if available via direct contact. Since hydrogen bonds are fairly weak they are constantly breaking and reforming even at ambient temperature. Because of the latter, in-situ temperature rise should reduce the number of hydrogen bonds between the  $\text{Si}_3\text{N}_4$  and polyimide as ring closure through regular dehydrolysis also becomes possible. This mechanism is consistent with the data, which shows a decrement in the interface tensile strength with increasing temperature. Also, this explains the irreversible degrading effect of one heating cycle, as fewer open rings would mean a fewer sites for the nitrogen from nitride to bond to the polyimide precursor.

The degrading effect of increasing relative humidity content and hold times is a direct result of the competition between the water molecules that segregate the interfacial region and the nitrogen of the nitride in forming the hydrogen bonds with the polyimide precursor. Whether the observed degradation in the strengths is a direct result of film swelling is a subject of on-going investigation. Similarly, it is of interest to see if the strength degradation during in-situ temperature testing can be explained by the temperature-dependent relaxation in the film modulus. Such tests are presently in progress.

### *The New Reliability Approach for Devices and Packages*

The development of above interface strength-measuring apparatuses now afford implementation of a novel device reliability strategy. The proposed approach involves measurement of the interface's *intrinsic* tensile strength and its degradation as a function of the interfacial moisture content and *in situ* temperature rise that occurs during processing of individual components (IC's and substrates) and system-level IC integration, for critical interfaces, in the blanket geometry. These interfaces are those where delaminations are typically observed in processing and in service. Once such "strength charts" are developed for varying humidity and temperature conditions, they are to be used in conjunction with the already well developed simulation codes that are capable of predicting time-dependent stress concentrations, moisture accumulation, and temperature rise at any of the interfaces within the package assembly, for determining (a) whether the interface will be able to survive processing and system integration cycles during the design phase itself, prior to any IC fabrication and packaging, and (b) the level of interface strength needed at the time of manufacturing for ensuring a *prescribed* service life. This value can be essentially obtained by first reading off the strength degradation corresponding to the calculated moisture accumulation over the desired service life from the charts, and then adding to it the largest stress concentration at the critical interface under expected service loads, as calculated from the FEM codes. In addition to being more rational, reliable, and robust, the proposed methodology should result in significant time and cost savings compared with the exhaustive set

of accelerated time/temperature/humidity tests that are presently employed by the industry. Needless to say, the above strategy can also be used to optimize geometries of new IC's, interconnections, and packages, during the design phase itself.

#### ***4.2.3. Effect of Film Thickness and Cure Temperature on the Cracking Behavior of Low-k Dielectric Films***

The purpose of this work performed in collaboration with Cow Corning Corporation was to provide an explanation for the rather dissimilar cracking phenomenon exhibited by the thin and thick hydrogen silsesquioxane (HSQ) dielectric films deposited on Si wafers. Specifically, films less than 1  $\mu\text{m}$  could be cured at 470°C for an unlimited time without cracking with tensile residual stresses in excess of 200 MPa, whereas their thicker counterparts (2  $\mu\text{m}$  and higher) cracked and delaminated spontaneously after entrapping a residual stress of only 20 MPa. So, why did thin films survive cracking and delamination even though they entrapped a strain energy density ( $\sim \sigma^2 t/E$ ) that was three times the value that resulted in the failure of thicker deposits? The laser spallation technique was used to investigate this phenomenon. The tensile strength of interfaces formed by thin films was found to be substantially higher (0.39-1.25 GPa) compared with those for the thicker deposits (11-71 MPa). This dissimilarity in the interface strength was found to be consistent with the increased ratio of 20 and higher for the SiO to SiH normalized bond densities, as determined by FTIR spectroscopy, in thin deposits compared with that of only 2.04 in the thicker films. Presumably an increase in the number of SiO bonds promotes the formation of Si-O-Si bonds across the interface with the underlying thermally-grown oxide layer on Si wafer and results in enhanced adhesion. Because SiO bonds are rather hard and inflexible, such chemical changes were also consistent with the measured Young's Modulus data; 5-16 GPa for the thin films vs. only 2 GPa for the thick ones. These results are presently being synthesized into manuscript [14].

#### **4.3. Technology Transfer**

Technology based on the laser spallation concept was developed, and fully transferred to Intel Corporation. Also, it was used for product development in companies worldwide, belonging not to one but different industries, such as semiconductor (Intel Corporation, Hitachi, Dow Corning Corporation), automobile (Delco), television (LG Gould in Korea), biomedical (Pacesetter Inc., Baxter Corporation), aircraft engines (Pratt and Whitney, Westinghouse Corporation), paint (Du Pont), and Dentistry (improved Ti implants with highly adherent calcium-phosphate coating). The usage is presently continuing, and negotiations are underway for full transfer of the technology to several companies.

Specific results are precluded because of propriety reasons. In general, while working with the semiconductor industry we have shown that the fundamental tensile strength of interfaces between thin polymeric layers and differently treated glass surfaces (with intervening layer of nitride) can be effectively measured using a laser spallation technique and that the technique is rather sensitive to the atomic and chemical structure of the interfacial region such that any small processing variations which affect these are readily picked up by the technique in terms of the variation in the measured tensile strength numbers. Since it takes only few seconds to do the test (once the conversion of the laser energy to the local interface stress is done via an optical interferometer for a given type of substrate), the technique can be used for quality control in the manufacturing environment, or for the development of new processes for improving adhesion.

We also tested adhesion at the Cu/dielectric, polyimide/silicon-nitride, polyimide/silicon oxide, and epoxy (used for underfill)/polyimide interfaces (a) in the blanket form where the above interfaces were deposited on a Si wafer, (2) as they appear in ICs and substrates before packaging, and (3) in ICs and substrates that were packaged using the traditional wire bond and the newer flip chip bonding processes. In (2), by moving the location of the laser-generated stress wave spot and its size (which can be varied anywhere from 3 mm to tens of microns) we were able to measure the adhesion between the polyimide and the nitride layers in the ICs that were fabricated with two to five levels of micro-circuitry (so called short and full loop Si devices). Similarly, adhesion between Cu vias/Cu lines, Cu lines/dielectric layer, Pb-Sn bumps and underlying Cu pads, were determined in C4 plastic packages.

The same approach was utilized in (3) for packaged ICs, where in addition to above interfaces in the IC and C4 packages, adhesion at additional and more critical (from reliability point of view) interfaces was tested. These included, interfaces between (a) the underfill and the polyimide layer on the IC (formed in the flip chip process), (b) between the underfill and the top surface of a plastic C4 substrate, (c) between the Sn-Pb solder and the underlying Cu pad on the substrate side, and (d) between the Pb-Sn solder and the metallic bond pads on the IC side. Remarkably, all of the above interfaces could be tested after the IC was packaged using the flip chip process.

A few accelerated humidity/temperature/time tests which are typically done in the industry and take several hours to perform were also done on all of the above interfaces, in blanket form, on individual ICs and substrates, and packaged ICs. Rather interestingly, the interface strength for all cases was found to be degraded, the magnitude of which was measured within few seconds by the laser spallation experiment. Thus, by forming a bridge between the spallation and the accelerated test results, a significant time saving was accomplished during product development and reliability testing. This experiment is expected to replace accelerated tests that are presently used for testing the mechanical reliability of devices.

Beside plastic packages and ICs that were packaged using the flip chip process, the spallation technology can work on different substrates (ceramic-based), and also packages manufactured using traditional approaches.

For the jet aircraft engine industry, we were able to provide strength results for PSZ coatings on superalloy substrates, for different process conditions. The work with Westinghouse Corporation also involved the use of laser ultrasound for characterizing subcritical interface cracks, as needed for inspecting turbine blades. None of these developments, however, led to any technology transfer.

#### **4.4. Contributions to other Fields**

##### **4.4.1 Biomedical**

We explored two new research frontiers in the area of Biomedical Engineering. In the first research, in collaboration with the Pediatric Cardiology Department at UCLA, we used larger-amplitude laser-generated acoustic pulses for the treatment of arrhythmias. The idea is to *temporarily* insulate a suspected conduction band by disrupting its intra cellular bonds by transmission of such stress pulses, before inactivating them permanently via microwave heating. This year activities involved surgically removing a section of the myocardium tissue from an

adult rabbit heart, and subjecting it to the acoustic pulses in the laser spallation assembly. Preliminary experiments have been quite encouraging. This research has exceptional promise as it may revolutionize the way in which arrhythmias are presently treated, where the suspected areas are burned permanently by microwave heating without a priori knowledge of its malignancy.

In a separate research, in collaboration with Dr. John Jansen of the University of Nijmegen in the Netherlands, special-stoichiometric Ca-PO coatings to which the natural bone growth process is accelerated were synthesized for titanium dental implants. These important findings are described in [15]. Both of the above applications are summarized schematically in Fig 16.

Recently a research project exploring the use of high frequency laser ultrasound for dissolution of body fat has been initiated.

#### **4.4.2 Dynamic Fracture/Geophysics**

A system for measuring the interface crack velocity was developed, and applied to photolithographically-generated 90-100  $\mu\text{m}$  long cracks between a thin (1  $\mu\text{m}$ ) Nb strip of 60  $\mu\text{m}$  width and a sapphire substrate. The cracks were loaded using a laser-generated stress wave. The duration of crack advance as needed for determining the average crack velocity was taken as the time during which the interface tensile stress exceeded that needed for crack initiation. This was numerically calculated using the interferometrically-measured free surface velocity of the sapphire as an input. Equi-spaced Al lines of 200  $\text{\AA}$  thickness were deposited in front of the crack tip using photolithography and used as markers to determine the total crack advance by viewing the shock-loaded samples in a scanning electron microscope. The maximum crack propagation speed of 11346 m/s was determined which is close the dilatational wave speed of 11090 m/s in the stiffer sapphire along its basal plane axis. These observations are the first report of crack speeds approaching the dilatational wave speed of the stiffer bimaterial component. These observations have significance to geophysical phenomenon of fault instability and indicates that faults can travel faster than the Rayleigh wave speed of the medium. The fact that the crack speed exceeds the second Rayleigh wave speed of the stiffer material is at unrest with most dynamic fracture frameworks. The results of the above investigation are schematically summarized in Fig. 17, with details found elsewhere [16].

#### **4.4.3. A fundamental Study of the Ice-Structure Adhesion Process**

A self-assembled monolayer (SAM) of dimethyl-n-octadecylchlorosilane was developed as a low ice adhesion surface for structural Al surfaces. The silane group reacted with the hydroxyl group on the Al surfaces to form a strong covalent Si to Al bond, while the other end of the chain was essentially hydrophobic. Ice was grown on the surface of the SAM and its interface strength measured using an updated version of the laser spallation apparatus equipped with an environmental chamber to perform strength measurements between  $-1^{\circ}\text{C}$  and  $-40^{\circ}\text{C}$ . The effect of Al surface roughness and other polymer layers on the adhesion of ice was also studied. Ice adhesion was found to be lowest (140 MPa) on the surface of SAM compared with other surfaces, e.g., for PI: 174 MPa, PMMA: 181 MPa, and bare Al: 274 MPa. Details can be found in [17].

## 5. List of Papers Published

Response to the Comments of Nutt and King on the Bond Strength Measurements of Gupta et al., A. S. Argon, J. A. Cornie, V. Gupta, L. Lev, and D. M. Parks, *Materials Science & Engineering*, Vol A237, pp. 224-228, 1997.

Effect of Substrate Orientation, Roughness and Film Deposition Mode on the Tensile Strength and Toughness of Niobium-Sapphire Interface, V. Gupta, Jianxin Wu and A. N. Pronin, *J. American Ceramic Society*, Vol. 80 (12), pp. 3172-3180, 1997.

Measurement of Thin Film Interface Toughness, A. N. Pronin and V. Gupta, *J. Mechanics and Physics of Solids*, Vol. 46 (3), pp. 389-410, 1998.

Measurement and Control of Ice Adhesion to Aluminum 6061 Alloy, Paul Archer and V. Gupta, *J. Mechanics and Physics of Solids*, vol. 46 910), pp. 1745-1771, 1998.

Measurement and Control of Interface Strength of RF Magnetron sputtered Ca-PO-Coatings on Ti-6Al-4V substrates by using the laser spallation technique, K. van Dijk, V. Gupta, A. K. Yu and J. A. Jansen, *J. Biomedical Materials Research*, Vol. 41, pp. 624-632, 1998.

Measurement of In-situ Fiber/Matrix Interface Strength in graphite/epoxy composites, A. Yu and V. Gupta, *Composites Science and Technology*, Vol. 58, pp. 1827-1837, 1998.

Measurement of Interface Tensile Strength at Elevated Temperatures, V. Gupta, M.O'Brien, and A. N. Pronin, *J. Phys. IV France*, Vol. 9, pp. 305-310, 1999.

Observations of Limiting Transonic Interface Crack Speeds, Jianxin Wu and V. Gupta, *J. Mechanics and Physics of Solids*, Vol. 48 (3), pp. 609-619, 2000.

A hydrophobic self assembled monolayer with improved adhesion to aluminum for deicing applications, B. Somlo and V. Gupta, *Mechanics of Materials*, in press.

Interfacial Adhesion and its Degradation in Selected Metal/Oxide and Dielectric/Oxide Interfaces in Multi-layer Devices, V. Gupta, R. Hernandez, J. Wu, and P. Charconnet, *Vacuum*, in press.

Effect of Humidity and Temperature on the Tensile Strength of Polyimide/Silicon Nitride Interface and its Implications for Electronic Device Reliability, V. Gupta, R. Hernandez, and P. Charconnet, *J. Materials Science and Engineering A*, in press.

The Asymptotic Field of a Crack Propagating in the Supersonic Regime along an Anisotropic Bimaterial Interface, J. Wu and V. Gupta, submitted to the *J. Mechanics and Physics of Solids*.

Effect of Film Thickness and Cure Temperature on the Cracking Behavior of Low-k Dielectric Films, V. Gupta, C. K. Saha, A. Yu, and K. Chung, in preparation.

Surface Science-Based Adhesion Enhancement Using A Laser Spallation technique, V. Gupta, in *Surface Engineering: Science and Technology I*, Edited by A. Kumar, Y.-W. Chung, J. J. Moore, and J. E. Smugeresky, The Minerals, Metals & Materials society, 1999, pp. 9-20.



Measurement of Interface Tensile Strength at Elevated Temperatures, V. Gupta, M.O'Brien, and A. N. Pronin, in *Proceedings of the 3<sup>rd</sup> European Mechanics of Materials Conference: EUROMECH-MECAMAT*, held Oxford-U.K., 23-25 Nov., 1998.

Tensile Strength of nitride/Polyimide Interface and Its Degradation due to Moisture Segregation with Implications for Device Reliability, V. Gupta, R. Hernandez, and P. Charconnet, in *Proceedings of the ISAPS'99: advances in Applied Plasma Science*, Vol. 2, 1999, pp. 343-350.

## **Reports**

[1] Characterizing fundamental adhesion in multilayer devices by using the laser spallation technique: Part I. Relative adhesion on polyimide/nitride/oxide multilayer blanket wafers, Si full and Short Loop Devices, and OLGA packages, with and without the precon Treatment. Report submitted to the Adhesion Working Group at Intel Corporation, Intel Corporation's Adhesion, June, 1998.

[2] Characterizing interfacial adhesion in multilayer devices by using the laser spallation technique Part-ii. (a) quantification of the interface tensile strengths in multilayer blanket structures with applications to polyimide/nitride/oxide/si interfaces, and (b) in-situ relative adhesion measurements at the underfill/die, underfill/substrate, Pb-Sn-bumps/bond-pads, and pb-sn-bumps/cu-via interfaces in packages and substrates. Report submitted to the Adhesion Working Group at Intel Corporation, August 1999.

## **6. List of Scientific Personnel Supported**

Jianxin Wu, Supported as a Ph.D. Student throughout and obtained Ph.D. in June, 1998.

Allen Yu, Finished MS Thesis, 1998.

Zheng Yi Jia, Laboratory Assistant, 1997-98.

Vassili Post Doctoral Research Fellow, 1998.

Vijay Gupta, Principal Investigator, throughout the project duration.

## 7. Bibliography

- [1]. V. Gupta, J. Yuan, and A. N. Pronin, *J. Adhes. Sci. Tech.* 8, 6 (1994) 713.
- [2]. J. Yuan, and V. Gupta, *Acta Metallurgica et Materialia*. 43, 2 (1995) 781.
- [3]. J. Yuan, V. Gupta, and M. Kim, *Acta Metallurgica et Materialia*. 43, 2 (1995) 769.
- [4]. A. S. Argon, J. A. Cornie, V. Gupta, L. Lev, and D. M. Parks, *Mat. Sci. and Eng. A237* (1997) 224.
- [5] Characterizing interfacial adhesion in multilayer devices by using the laser spallation technique Part-ii. (a) quantification of the interface tensile strengths in multilayer blanket structures with applications to polyimide/nitride/oxide/si interfaces, and (b) in-situ relative adhesion measurements at the underfill/die, underfill/substrate, Pb-Sn-bumps/bond-pads, and pb-sn-bumps/cu-via interfaces in packages and substrates. Report submitted to the Adhesion Working Group at Intel Corporation, August 1999.
- [6] V. Gupta, M. O'Brien, and A. N. Pronin, *J. Phys. IV France*. 9 (1999) 305.
- [7] P. Archer, and V. Gupta, *J. Mech. Phys. Solids*. 46, 3 (1998) 389.
- [8] A.S. Argon, V. Gupta, H.S. Landis, and J. A. Cornie, *Mater. Sci. Engg.* 24 (1989) 41.
- [9] V. Gupta and A. N. Pronin, *J. Amer. Ceram. Soc.* 78, 5 (1995) 1397.
- [10]. A. N. Pronin, and V. Gupta, *J. Mech. Phys. Solids*. 46, 3 (1998) 389.
- [11]. V. Gupta, J. Wu, and A. N. Pronin, *J. Amer. Ceram. Soc.* 80, 12 (1997) 3172.
- [12] Interfacial Adhesion and its Degradation in Selected Metal/Oxide and Dielectric/Oxide Interfaces in Multi-layer Devices, V. Gupta, R. Hernandez, J. Wu, and P. Charconnet, *Vacuum*, in press.
- [13] Effect of Humidity and Temperature on the Tensile Strength of Polyimide/Silicon Nitride Interface and its Implications for Electronic Device Reliability, V. Gupta, R. Hernandez, and P. Charconnet, *J. Materials Science and Engineering A*, in press.
- [14] Effect of Film Thickness and Cure Temperature on the Cracking Behavior of Low-k Dielectric Films, V. Gupta, C. K. Saha, A. Yu, and K. Chung, in preparation.
- [15] K. van Dijk, V. Gupta, A. K. Yu, J. A. Jansen, *J. Biomed. Mater. Res.* 41 (1998) 624.
- [16] J. Wu and V. Gupta, *J. Mechanics and Physics of Solids*. 48, 3(2000) 609.
- [17]. B. Somlo and V. Gupta, *Mech. Mater.* in press.

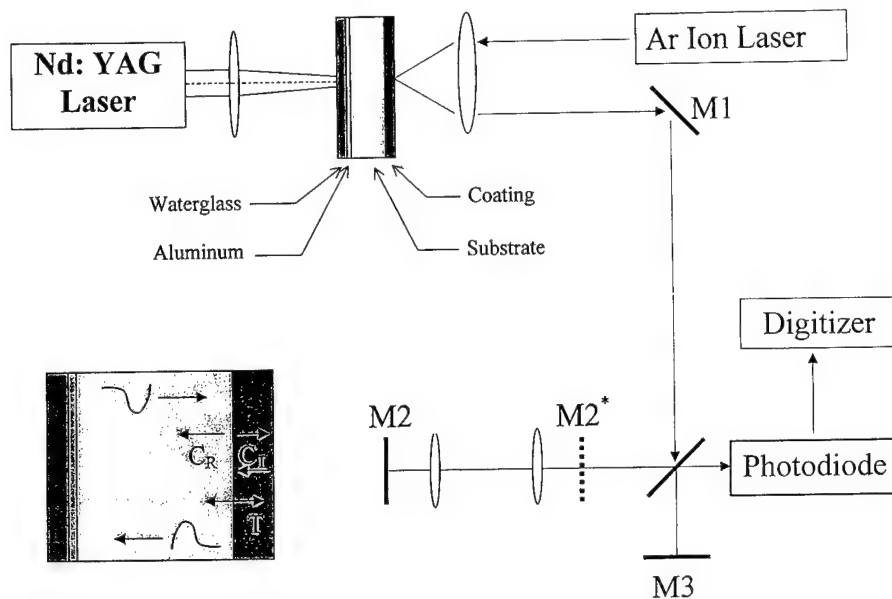


Figure 1

Relative Time (ns)

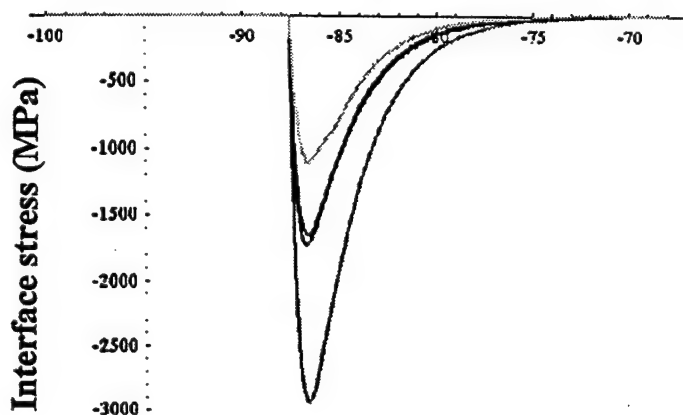


Figure 2

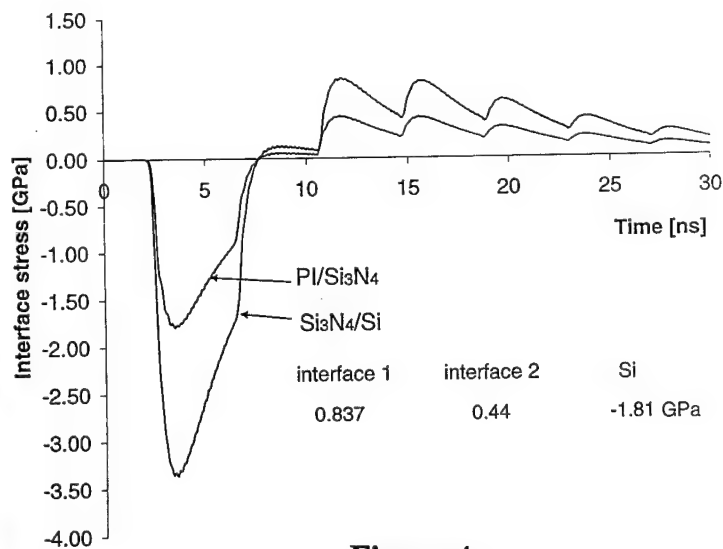


Figure 4

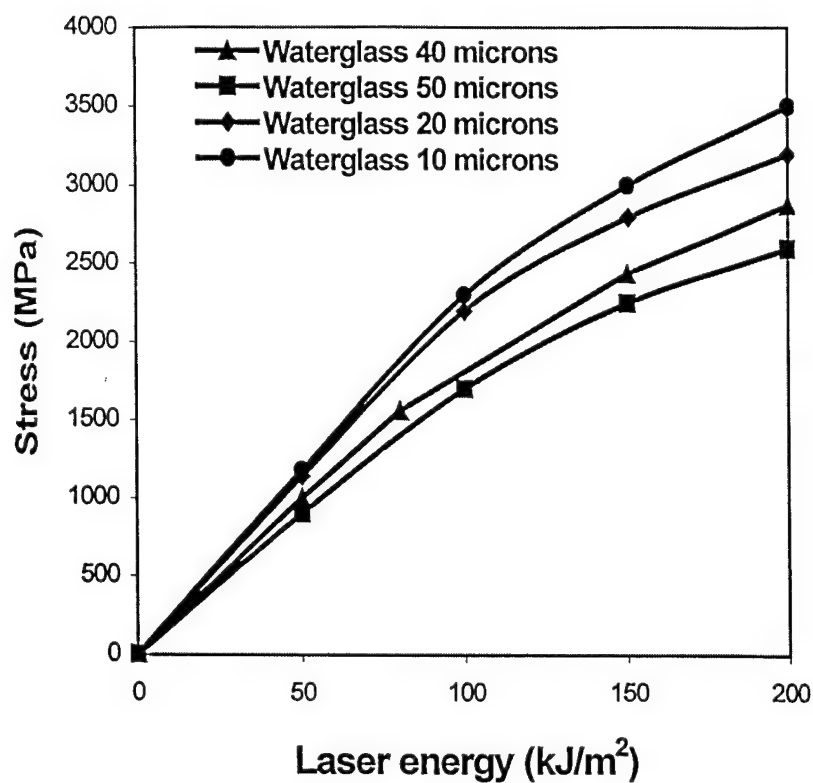
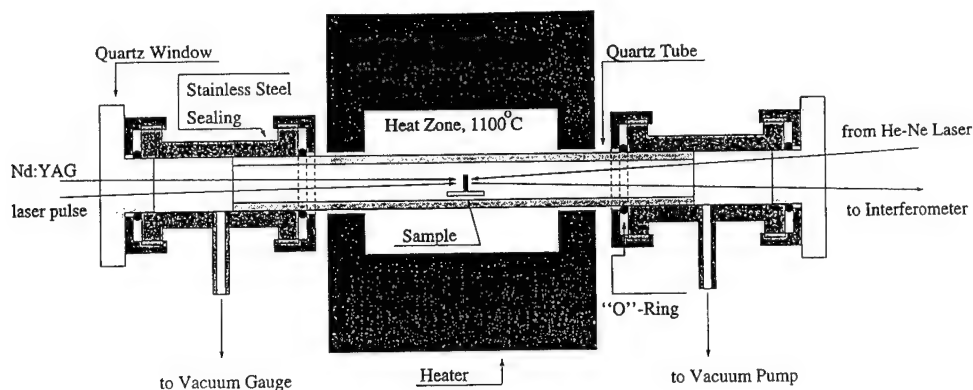


Figure 3



**Figure 5**

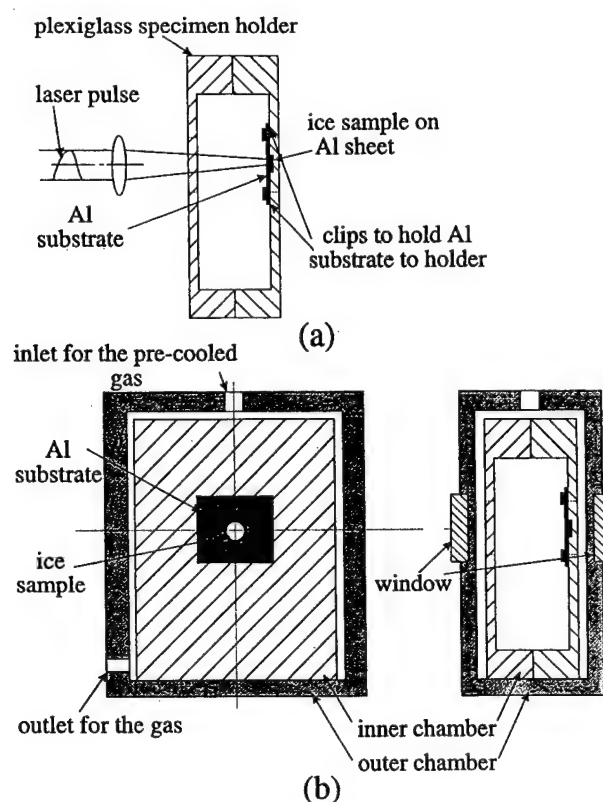


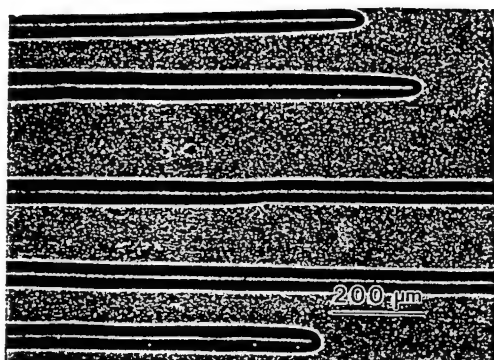
Fig. 6. A schematic diagram of the ice sample holder used in the aluminum-ice adhesion experiments: (a) inner chamber; (b) outer chamber.

**Figure 6**

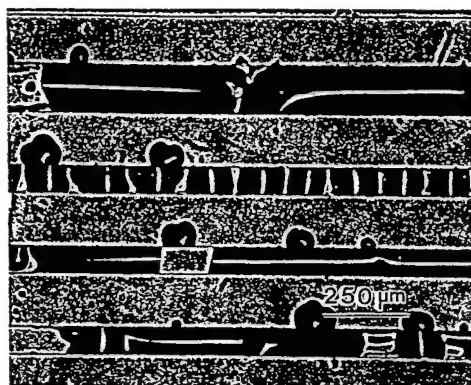
Table 2. Results for the laser spallation experiments on the Al-ice interface system with various aluminum surface treatments

Substrate Surface	Temp (°C)	Interface strength (MPa)	No. of experiments
Unpolished Al	-10	274 ± 17.1	6
Unpolished Al	-20	192	4
Unpolished Al	-30	183	6
Unpolished Al	-40	179	5
Polished Al	-10	180.8 ± 6.4	8
Al + 1 μm PMMA	-10	190.3 ± 8.0	8
Al + 1 μm PI	-10	181	5

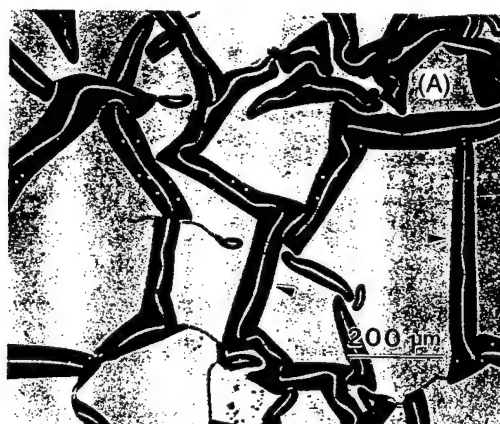
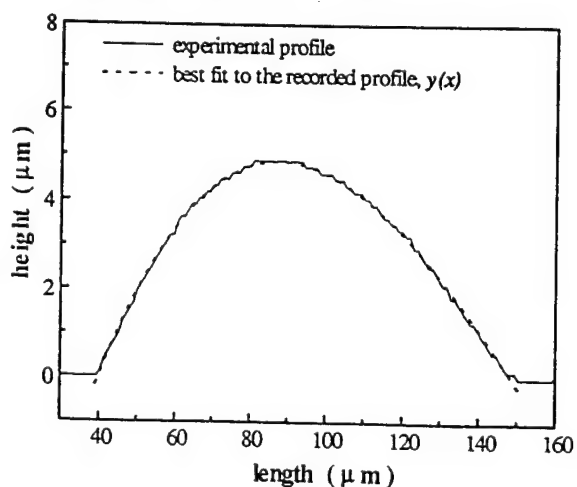
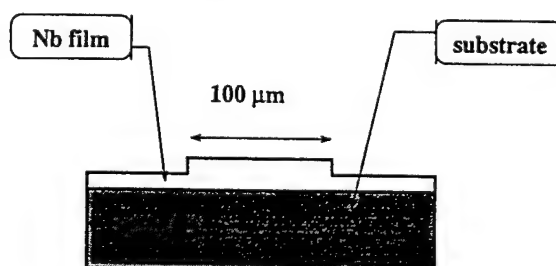
All temperatures shown for the experiments are  $\pm 1^\circ\text{C}$ . The number of experiments in which interface damage was observed at the indicated stress is shown after the stress.



Naturally-occurring straight-edge one-dimensional buckled profiles



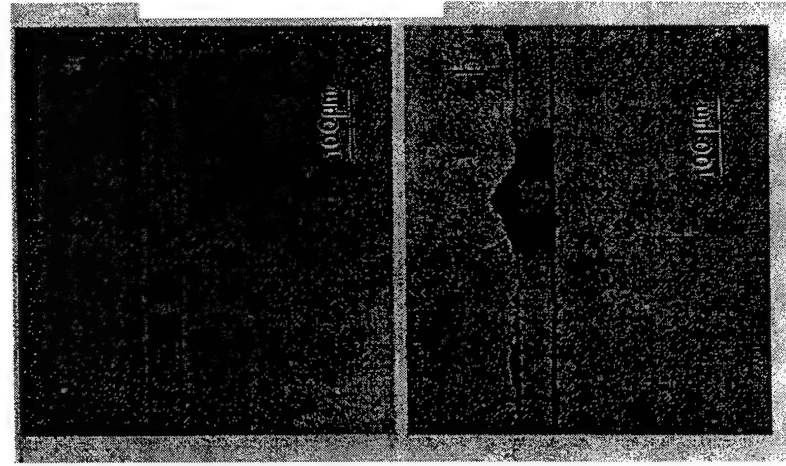
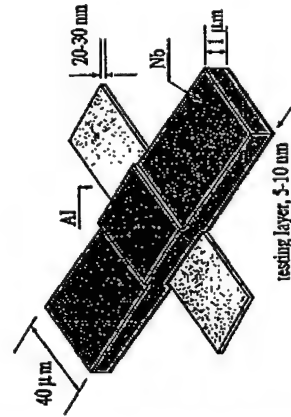
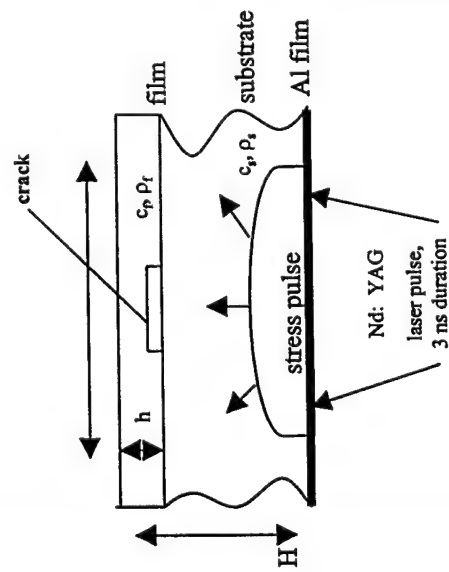
A micrograph showing one-dimensional buckled morphologies in Nb coating deposited using the photolithographic techniques.



A one-dimensional post-buckled profile of the Nb film obtained from a mechanical profilometer. The dotted line represents a polynomial fit to the measured profile.

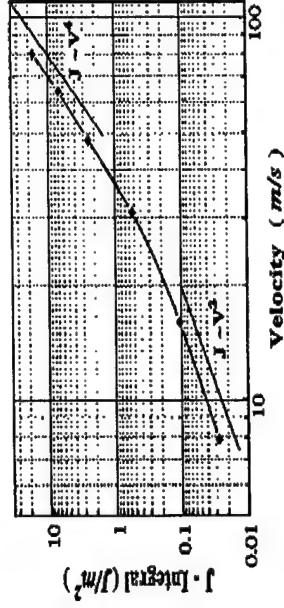
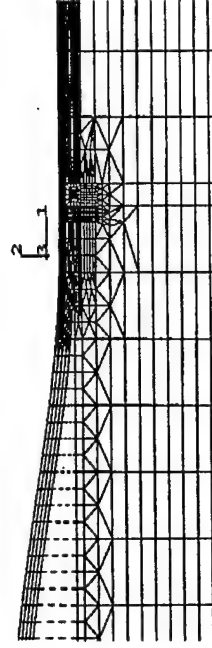
Figure 7

# Measurement of Thin Film Interface Toughness by Using Laser-Generated Stress Pulses



a - before loading

b - after loading



*Toughness of several metal/sapphire interfaces as obtained by the new dynamic stress pulse technique and the spontaneous delamination experiment*

Interface systems	Critical Nb Film thickness ( $\mu\text{m}$ )	Interface toughness from the spontaneous delamination technique (Gupta and Pronin, 1995) ( $\text{J/m}^2$ )	Dynamic $J$ -integral values at crack initiation ( $\text{J/m}^2$ )	Critical velocity amplitude at crack initiation ( $\text{m/s}$ )
Al/sapphire	$1.0 \pm 0.05$	$1.03 \pm 0.05$	1.3	42
Sb/sapphire	$0.3 \pm 0.03$	$0.31 \pm 0.03$	0.04	10
Nb/sapphire	$0.85 \pm 0.05$	$0.88 \pm 0.05$	0.6	24
Cr/sapphire	$0.91 \pm 0.05$	$0.94 \pm 0.05$	0.8	27

Figure 8



# Effect of Substrate Orientation, Roughness, and Film Deposition Mode on the Tensile Strength and Toughness of Niobium-Sapphire Interfaces

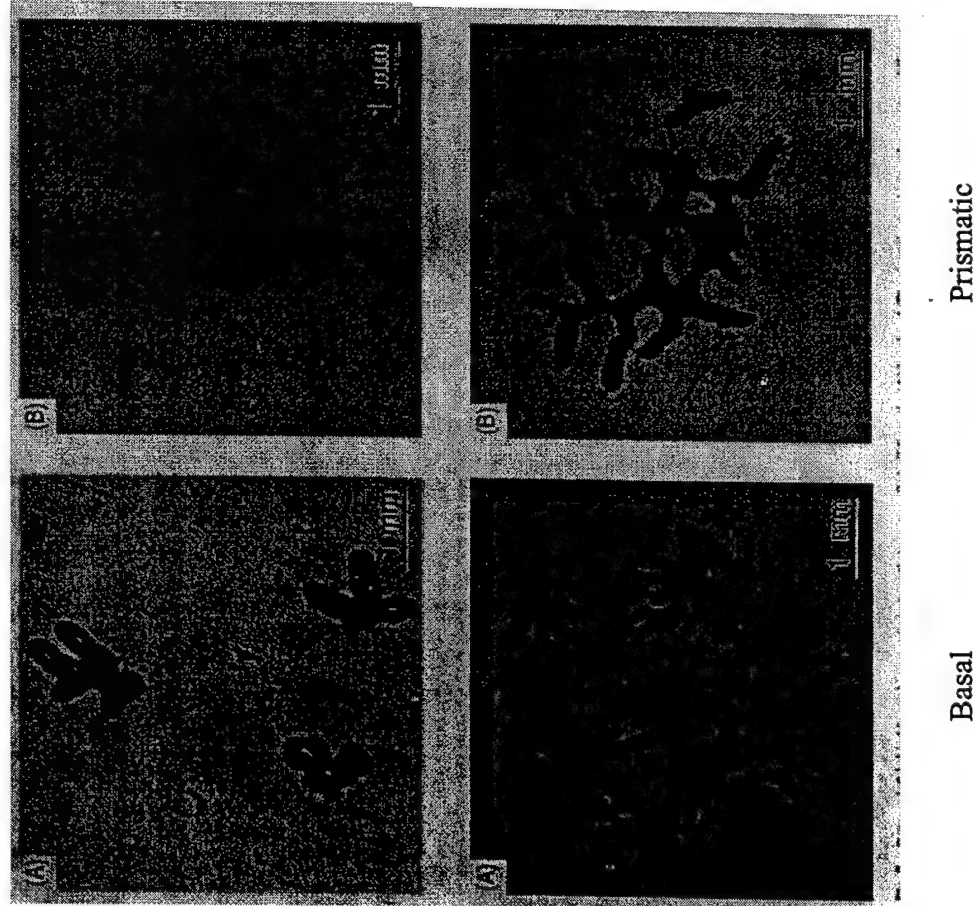


Figure 9

Tensile Strength Range\* as Measured by the Laser Spallation Technique for Several Niobium-Sapphire Interfaces of Varying Structure and Chemistry

Sapphire surface	Tensile strength (GPa)		Backsputtered mode
	dc mode	rf mode	
Basal	$0.38-0.79 \pm 0.03$	$0.45-0.97 \pm 0.08$	$0.52-1.30$
Prismatic	$0.57-0.98 \pm 0.06$	$0.66-1.17 \pm 0.01$	$0.53-1.40$

\* Error range corresponds to high threshold strength

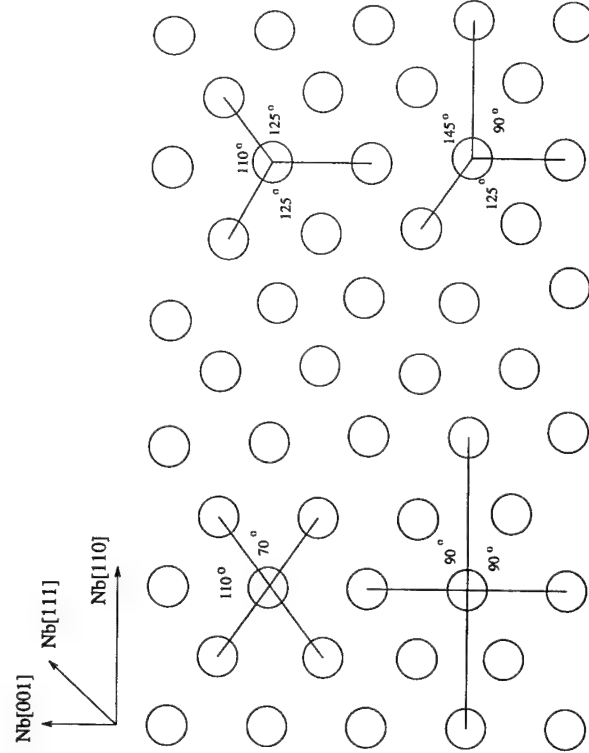


Fig. 8. Possible directions on a niobium-prismatic sapphire interface along which the niobium coating can decohere, as suggested by a two-dimensional atomic arrangement for an assumed interface structure. This is compared with the experimentally observed spallation patterns shown in Fig. 7.

Table 1. Tensile Strength of Interfaces Between Metallic Coatings and Silicon Substrates

Film	Substrate	Interface Tensile Strength in GPa
W	Si	0.11
Cu	Si	0.48
Cu	Si/SiO <sub>2</sub> with 0 min sputter etch	0.73
Cu	Si/SiO <sub>2</sub> with 3 min sputter etch	0.32
Cu	Si/SiO <sub>2</sub> with 10 min sputter etch	0.62

Figure 10

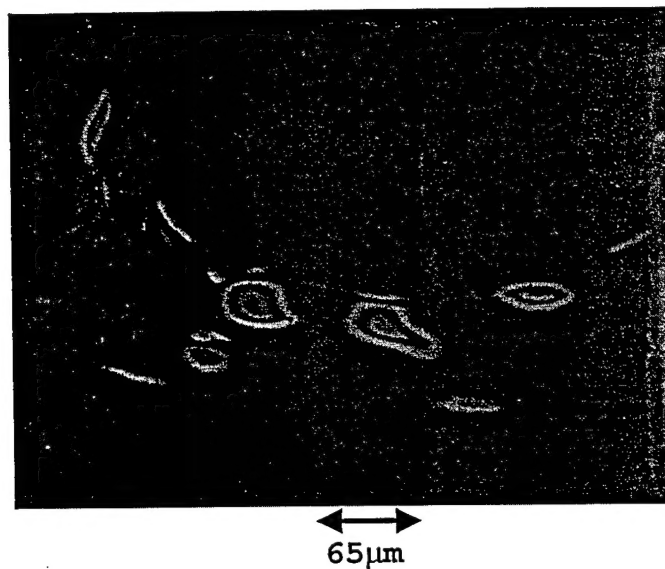


Figure 11

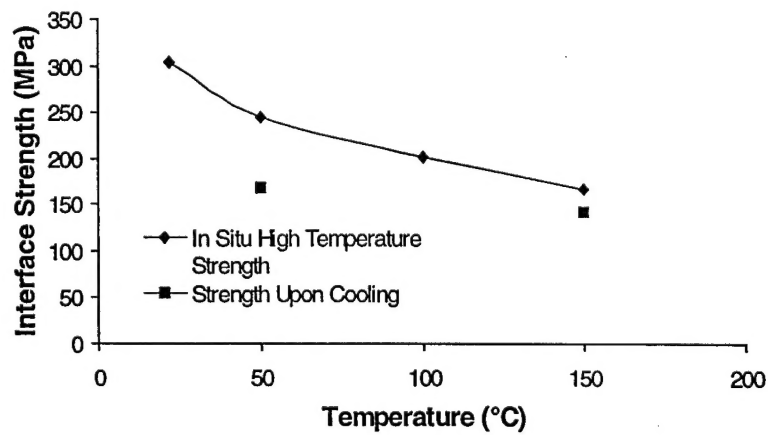


Figure 12

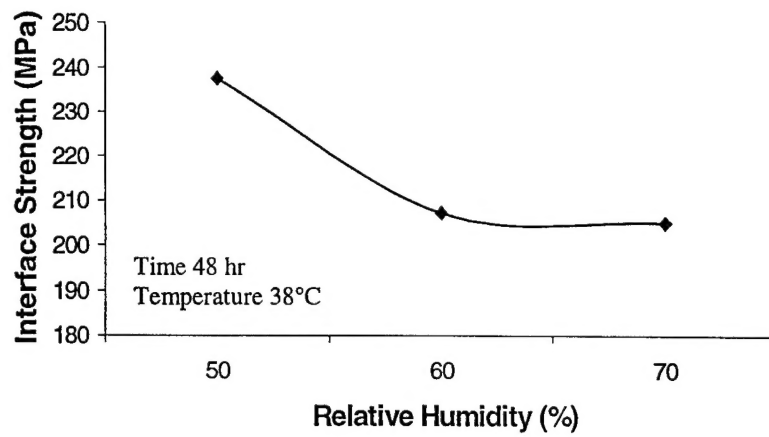


Figure 13

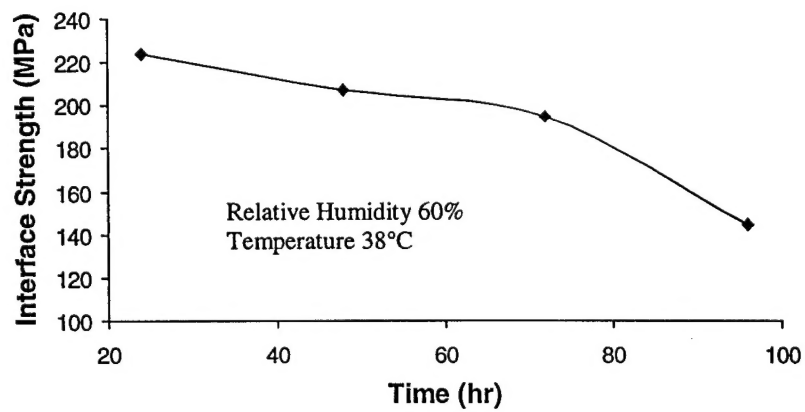


Figure 14

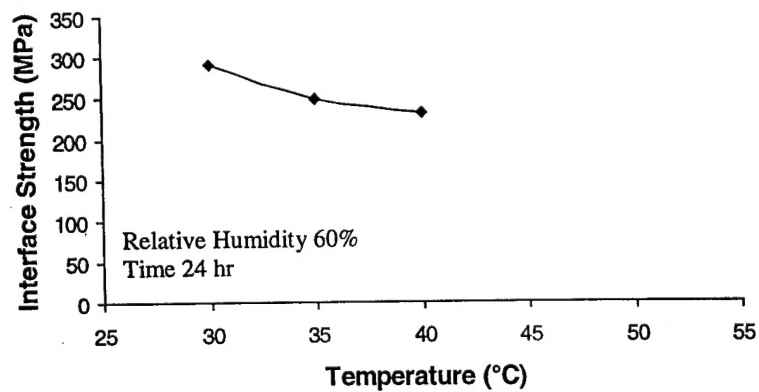
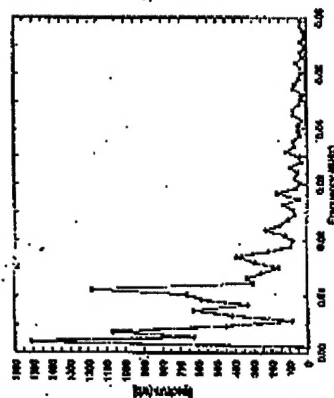
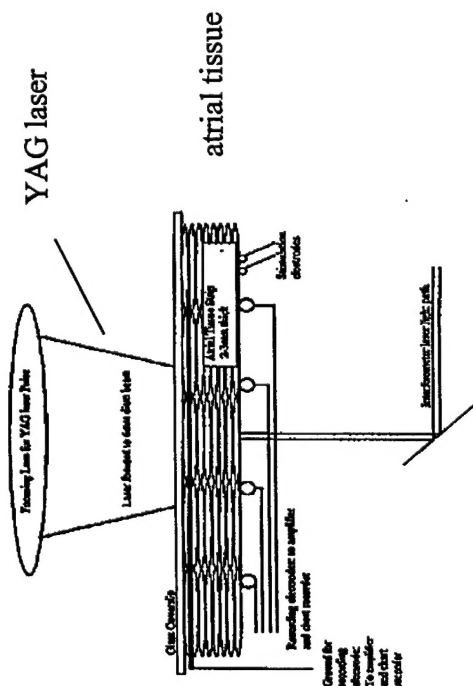


Figure 15

# Improving Adhesion of Calcium Phosphate Coating on Ti Dental Implants

## Treatment of Arrhythmia



**Fig. 7**  
Frequency spectrum of a transmitted stress wave signal

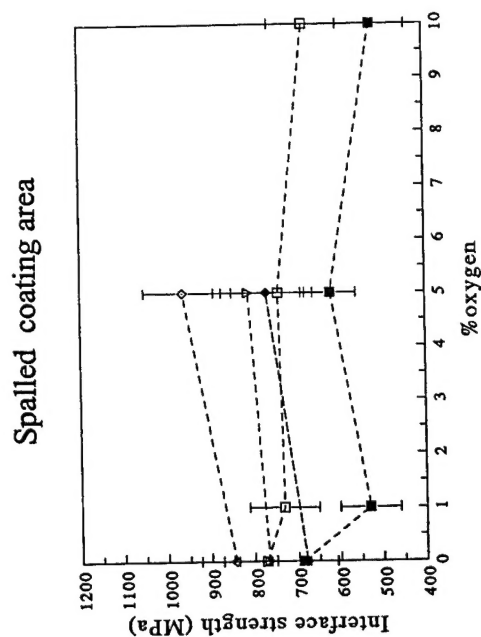
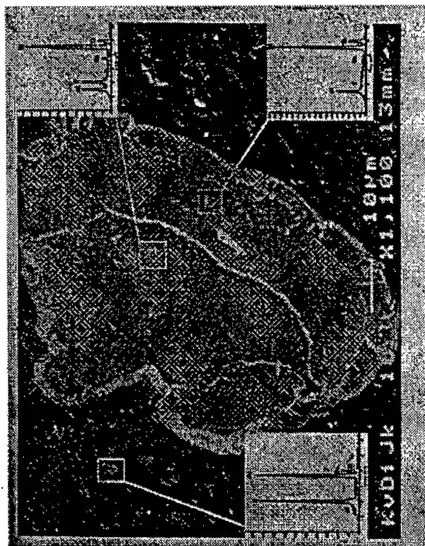
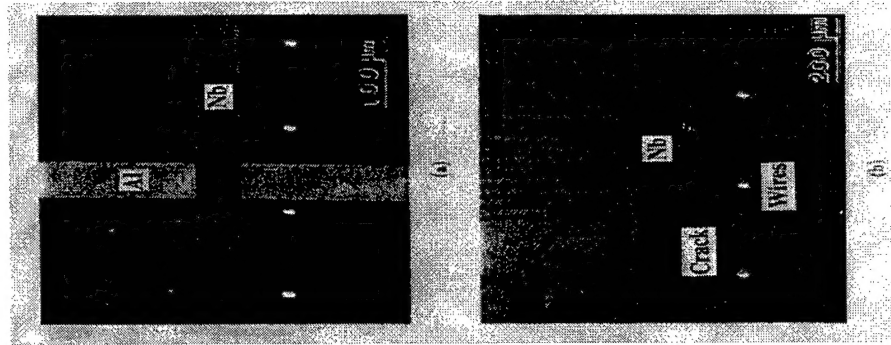
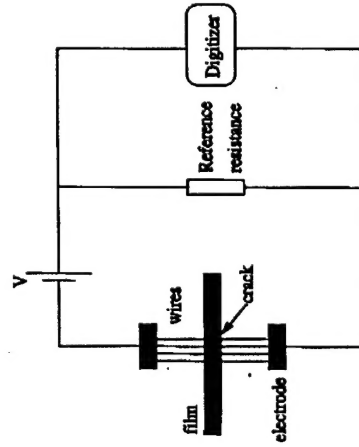


**Figure 8.** Interface strength versus partial oxygen pressure for films deposited at (■) 400 W  $1.5 \times 10^{-2}$  mbar rotating substrate holder, (□) 400 W  $1.5 \times 10^{-2}$  mbar indexed substrate holder, (▽) 200 W,  $3.0 \times 10^{-3}$  mbar, (◆) 200 W,  $1.5 \times 10^{-2}$  mbar, and (◇) 200 W,  $1.5 \times 10^{-2}$  mbar and 5 W bias. Error bars represent standard deviations.

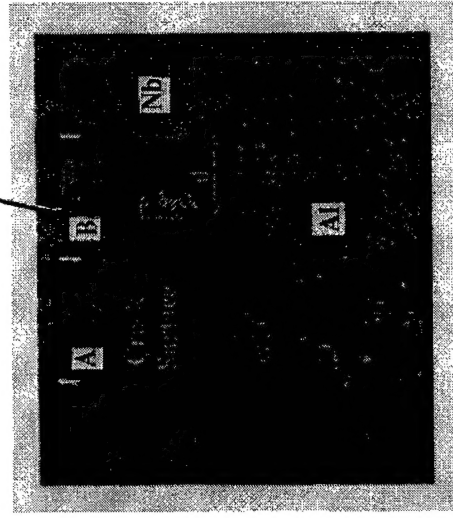
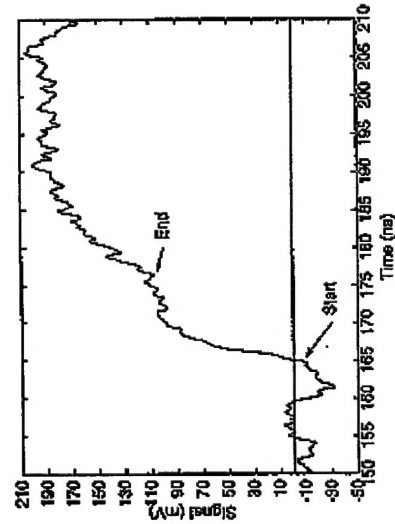
# Measurement of Interface Crack Velocity and an Apparatus for Studying Interaction Between Crack-tip and Active Materials Force Fields



Sample design for observation of interfacial crack propagation in thin film structures. (a) A  $1\ \mu\text{m}$  niobium stripe is overlaid on a  $200\ \text{\AA}$  aluminum under-sacrificial layer. The removal of the aluminum under-sacrificial layer by wet etch creates a microcrack; (b) aluminum wires of thickness  $200\ \text{\AA}$  are patterned at the crack tip to monitor the crack propagation during dynamic fracture tests.



circuit



## Results

Interface crack velocity at  
Nb/Sapphire Interface =  $11,346\ \text{m/sec}$   
Raleigh wave speed in  
sapphire =  $5693\ \text{m/s}$

Figure 17